

Studies of the Electric Dipole Transition of Deformed Rare-earth nuclei

H.Y.Ji¹, G.L.Long^{1,2,3*}, E. G. Zhao^{1,2} and S. W. Xu⁴

¹*Department of Physics, Tsinghua University, Beijing 100084, China*

²*Institute of Theoretical Physics, Chinese Academy of Sciences, Beijing, China*

³*Center of Theoretical Nuclear Physics, National Laboratory
of Heavy Ion Accelerator, Chinese Academy of Sciences, Lanzhou, 730000, P R China*

⁴*Institute of Modern Physics, Chinese Academy of Sciences, Lanzhou, 730000, P. R.
China*

(February 9, 2008)

Abstract

Spectrum and electric dipole transition rates and relative intensities in $^{152-154}\text{Sm}$, $^{156-160}\text{Gd}$, $^{160-162}\text{Dy}$ are studied in the framework of the interacting boson model with s,p,d,f bosons. It is found that E1 transition data among the low-lying levels are in good agreement with the SU(3) dynamical symmetry of the spdf interacting boson model proposed by Engel and Iachello to describe collective rotation with octupole vibration. These results show that these nuclei have SU(3) dynamic symmetry to a good approximation. Also in this work many algebraic expressions for electric dipole transitions in the SU(3) limit of the spdf-IBM have been obtained. These formulae together with the formulae given previously exhaust nearly all the E1 transitions for low-lying negative parity states. They are useful in analyzing experimental data.

Typeset using REVTeX

*Corresponding author: Gui Lu Long, Department of Physics, Tsinghua University, Beijing, 100084, P. R. China. Email: gllong@mail.tsinghua.edu.cn

Keyword: spdf interacting boson model, electric dipole transition, octupole vibration, SU(3) dynamical symmetry

I. INTRODUCTION

There have been intensive interests in the studies of octupole degree of freedom in nuclear structure recently both experimentally [1–9] and theoretically [10–27].

In the boson model, negative parity states are described by the spdf interacting boson model [10–12,14,13,16,17,19–21,28] or the sdf-IBM [22–26]. Otsuka [14] showed microscopically that p and f bosons are important in the low-lying negative parity states of even-even nuclei. The spdf IBM has been successful in the description of negative parity states in the Ba and rare-earth region [17,19,20]. The advantages of the algebraic approach is that it offers analytical expressions for the energy levels, electromagnetic transitions and many other quantities. The prediction and later experimental confirmation of the O(6) limit has been a well-known example of the success of the IBM [29].

The spdf IBM SU(3) limit is a dynamical symmetry describing octupole vibration in deformed nuclei proposed by Engel and Iachello [12,13]. It has been pointed that ^{232}U or other actinide nuclei may be candidates for the SU(3) limit [12,13,16]. While the spectrum agrees with the theoretical calculation very well, there are very few electromagnetic transition data. Thus it is difficult to check on the validity of the dynamic symmetry properties, in particular on the electric dipole transitions connecting positive and negative parity states. This is because finding nucleus with both good rotational feature in spectrum and with ample data of electric dipole transition is difficult. Besides, in real nucleus dynamical symmetry is usually somehow broken, for instance, even one of the best candidate of the sdg IBM SU(3) dynamic symmetry has some degree of symmetry-breaking [30]. But dynamic symmetries are very useful even though they are broken. They can be used to classify states and characterize the collective features of a nucleus. To a given nucleus near a dynamical symmetry, at first the gross structure is dictated by the dynamical symmetry. Then detailed structure of the nucleus can be attributed to symmetry breaking, and its description is the task of a more elaborate study. In addition, the dynamical symmetries can be used as landmarks in the nuclear chart table to classify typical collective motions, and other vast majority of nuclei can be put into categories of transition between two dynamical symmetries. Such a scheme is very successful in the descriptions of the positive low-lying states of even-even nuclei [31]. In this work we have studied the negative parity states of the rare-earth nuclei, namely $^{152-154}\text{Sm}$, $^{156-160}\text{Gd}$, $^{160-162}\text{Dy}$ using the SU(3) limit of the spdf interacting boson model. These nuclei are deformed and have ample data of electric dipole transition. We have found in this work that to a good approximation, the structure of these rare-earth nuclei can be well described by the SU(3) limit of the spdf interacting boson model. The paper is organized in the following. In section II, we give a brief description of the model and the necessary expressions of electric dipole transitions. In section III, we apply the results to ^{152}Sm on the spectrum and E1 transitions. In

section IV, we study other deformed rare-earth nuclei. Finally we give a discussion and a summary in section V.

II. THE MODEL

A. The energy eigenvalues

The energy eigenvalues have been discussed in Ref. [12,17]. In the SU(3) limit, the group chain can be written as

$$\begin{array}{ccccccc} U(16) \supset U(6) \otimes U(10) \supset SU_{sd}(3) \otimes SU_{pf}(3) \supset SU_{spdf}(3) \supset O(3) \\ n \quad n_+ \quad n_- \quad (\lambda_+ \mu_+) \quad (\lambda_- \mu_-) \quad (\lambda \mu) \quad L, \end{array} \quad (1)$$

the energy eigenvalue is

$$E = \epsilon_- N_{pf} + a_1 C_{2SU_+} + a_2 C_{2SU_-} + a_3 C_{2SU(3)} + a_4 L(L+1). \quad (2)$$

The g.s.-band, β -band and γ -band are generated from $(2n, 0)$, $(2n-4, 2)K=0$ and $(2n-4, 2)K=2$ respectively, with n sd-bosons. The low-lying negative parity are generalized by the SU(3) IR from the decomposition of $(2n, 0) \otimes (3, 0)$; that is $K^\pi = 0^-$ from $(2n+3, 0)$ and $K^\pi = 1^-$ from $(2n+1, 1)$ respectively. For the low-lying states, we are interested in only the g.s., β , $\gamma, 0^-$ and 1^- bands.

The wave function are given by

$$\begin{aligned} (1) & \text{ground state band } |(2n, 0)_+ LM\rangle, \\ (2) & \beta \text{ band } |(2n-4, 2)_+ K=0 LM\rangle, \\ (3) & \gamma \text{ band } |(2n-4, 2)_+ K=2 LM\rangle, \\ (4) & K^\pi = 0^- \text{ - band } |(2n-2, 0)_+ (3, 0)_- (2n+1, 0) LM\rangle, \\ (5) & K^\pi = 1^- \text{ - band } |(2n-2, 0)_+ (3, 0)_- (2n-1, 1) LM\rangle. \end{aligned} \quad (3)$$

The value of a_2 is taken zero, since its effect in the spectrum is the same as that of ϵ_- term for the low-lying states with only one pf-boson. The parameters are then determined by experimental data.

B. The E1 transition matrix elements

Some of the E1 transition formulae have been given in Ref. [28]. With the method described there, we calculate the following formulae for the E1 transition, which are needed for a comparison with experiment, and the required SU(3) Wigner coefficients can be found in Ref. [32,33].

(a) $(2n+3, 0)K=0 \ L^- \rightarrow (2n-2, 2)K=0 \ (L-1)^+$ transitions, e.g. $1^- \rightarrow 0^+$,

$$\begin{aligned} \langle (L-1)^+ | (s^\dagger \tilde{p} + p^\dagger \tilde{s})^1 | L^- \rangle &= \frac{1}{(2n+1)} \times \\ &\sqrt{\frac{(2n-L+3)(2n+L+2)(2n+L+4)L \varphi(2n-1, L-1)}{20n(2n+3)}}, \end{aligned} \quad (4)$$

where

$$\varphi(\lambda, L) = 2(\lambda + 1)^2 - L(L + 1), \quad (5)$$

$$\begin{aligned} \langle (L - 1)^+ | (d^\dagger \tilde{p} + p^\dagger \tilde{d})^1 | L^- \rangle &= \frac{8n^2 - L(L - 1)}{5(2n + 1)} \times \\ &\sqrt{\frac{(2n - L + 3)(2n + L + 2)(2n + L + 4)L}{4n(2n + 3) \varphi(2n - 1, L - 1)}}, \end{aligned} \quad (6)$$

$$\begin{aligned} \langle (L - 1)^+ | (d^\dagger \tilde{f} + f^\dagger \tilde{d})^1 | L^- \rangle &= -\frac{8n^2 - L(L - 1)}{5(2n + 1)} \times \\ &\sqrt{\frac{3(2n - L + 3)(2n + L + 2)(2n + L + 4)L}{28n(2n + 3) \varphi(2n - 1, L - 1)}}. \end{aligned} \quad (7)$$

(b) $(2n+3,0)K=0 \ L^- \rightarrow (2n-2,2)K=0 \ (L+1)^+$ transitions, e.g. $1^- \rightarrow 2^+$,

$$\begin{aligned} \langle (L + 1)^+ | (s^\dagger \tilde{p} + p^\dagger \tilde{s})^1 | L^- \rangle &= -\frac{1}{(2n + 1)} \times \\ &\sqrt{\frac{(2n - L + 1)(2n - L + 3)(2n + L + 4)(L + 1) \varphi(2n - 1, L + 1)}{20n(2n + 3)}}, \end{aligned} \quad (8)$$

$$\begin{aligned} \langle (L + 1)^+ | (d^\dagger \tilde{p} + p^\dagger \tilde{d})^1 | L^- \rangle &= -\frac{8n^2 - (L + 1)(L + 2)}{5(2n + 1)} \times \\ &\sqrt{\frac{(2n - L + 1)(2n - L + 3)(2n + L + 4)(L + 1)}{4n(2n + 3) \varphi(2n - 1, L + 1)}}, \end{aligned} \quad (9)$$

$$\begin{aligned} \langle (L + 1)^+ | (d^\dagger \tilde{f} + f^\dagger \tilde{d})^1 | L^- \rangle &= \frac{8n^2 - (L + 1)(L + 2)}{5(2n + 1)} \times \\ &\sqrt{\frac{3(2n - L + 1)(2n - L + 3)(2n + L + 4)(L + 1)}{28n(2n + 3) \varphi(2n - 1, L + 1)}}. \end{aligned} \quad (10)$$

(c) $(2n+3,0)K=0 \ L^- \rightarrow (2n-2,2)K=2 \ (L-1)^+$ transitions, e.g. $3^- \rightarrow 2^+$,

$$\langle (L - 1)^+ | (s^\dagger \tilde{p} + p^\dagger \tilde{s})^1 | L^- \rangle = 0, \quad (11)$$

$$\langle (L - 1)^+ | (d^\dagger \tilde{p} + p^\dagger \tilde{d})^1 | L^- \rangle = 0, \quad (12)$$

$$\langle (L - 1)^+ | (d^\dagger \tilde{f} + f^\dagger \tilde{d})^1 | L^- \rangle = 0. \quad (13)$$

(d)(2n+3,0)K=0 $L^- \rightarrow (2n-2,2)K=2 L^+$ transitions, e.g. $3^- \rightarrow 3^+$,

$$\langle L^+ || (s^\dagger \tilde{p} + p^\dagger \tilde{s})^1 || L^- \rangle = 0, \quad (14)$$

$$\langle L^+ || (d^\dagger \tilde{p} + p^\dagger \tilde{d})^1 || L^- \rangle = 0, \quad (15)$$

$$\langle L^+ || (d^\dagger \tilde{f} + f^\dagger \tilde{d})^1 || L^- \rangle = 0. \quad (16)$$

(e)(2n+3,0)K=0 $L^- \rightarrow (2n-2,2)K=2 (L+1)^+$ transitions, e.g. $1^- \rightarrow 2^+$,

$$\langle (L+1)^+ || (s^\dagger \tilde{p} + p^\dagger \tilde{s})^1 || L^- \rangle = 0, \quad (17)$$

$$\langle (L+1)^+ || (d^\dagger \tilde{p} + p^\dagger \tilde{d})^1 || L^- \rangle = 0, \quad (18)$$

$$\langle (L+1)^+ || (d^\dagger \tilde{f} + f^\dagger \tilde{d})^1 || L^- \rangle = 0. \quad (19)$$

(f)(2n+1,1)K=1 $L^- \rightarrow (2n+2,0)K=0 (L-1)^+$ transitions, e.g. $1^- \rightarrow 0^+$,

$$\begin{aligned} \langle (L-1)^+ || (s^\dagger \tilde{p} + p^\dagger \tilde{s})^1 || L^- \rangle &= -\frac{(2n-3L+3)(2n+L+2)}{(2n+1)} \times \\ &\sqrt{\frac{(2n-L+3)(L+1)}{60n(2n+3)}}, \end{aligned} \quad (20)$$

$$\begin{aligned} \langle (L-1)^+ || (d^\dagger \tilde{p} + p^\dagger \tilde{d})^1 || L^- \rangle &= -\frac{4n^2 + 2(4L+5)n - 3(L-1)(L+2)}{5(2n+1)} \times \\ &\sqrt{\frac{(2n-L+3)(L+1)}{12n(2n+3)}}, \end{aligned} \quad (21)$$

$$\begin{aligned} \langle (L-1)^+ || (d^\dagger \tilde{f} + f^\dagger \tilde{d})^1 || L^- \rangle &= -\frac{16n^2 + 12Ln + 3(L-1)(L+2)}{5(2n+1)} \times \\ &\sqrt{\frac{(2n-L+3)(L+1)}{28n(2n+3)}}. \end{aligned} \quad (22)$$

(g)(2n+1,1)K=1 $L^- \rightarrow (2n+2,0)K=0 L^+$ transitions, e.g. $2^- \rightarrow 2^+$,

$$\langle L^+ || (s^\dagger \tilde{p} + p^\dagger \tilde{s})^1 || L^- \rangle = -\frac{(2n-L+2)(2n+L+3)}{(2n+1)} \sqrt{\frac{2L+1}{60n}}, \quad (23)$$

$$\langle L^+ || (d^\dagger \tilde{p} + p^\dagger \tilde{d})^1 || L^- \rangle = -\frac{(2n-L+2)(2n+L+3)}{5(2n+1)} \sqrt{\frac{2L+1}{12n}}, \quad (24)$$

$$\langle L^+ || (d^\dagger \tilde{f} + f^\dagger \tilde{d})^1 || L^- \rangle = -\frac{16n^2 + (L-2)(L+3)}{5(2n+1)} \sqrt{\frac{2L+1}{28n}}. \quad (25)$$

(h) $(2n+1,1)K=1 \ L^- \rightarrow (2n+2,0)K=0 \ (L+1)^+$ transitions, e.g. $1^- \rightarrow 2^+$,

$$\begin{aligned} \langle (L+1)^+ || (s^\dagger \tilde{p} + p^\dagger \tilde{s})^1 || L^- \rangle &= -\frac{(2n-L+1)(2n+3L+6)}{(2n+1)} \times \\ &\sqrt{\frac{(2n+L+4)L}{60n(2n+3)}}, \end{aligned} \quad (26)$$

$$\begin{aligned} \langle (L+1)^+ || (d^\dagger \tilde{p} + p^\dagger \tilde{d})^1 || L^- \rangle &= -\frac{4n^2 - 2(4L-1)n - 3(L-1)(L+2)}{5(2n+1)} \times \\ &\sqrt{\frac{(2n+L+4)L}{12n(2n+3)}}, \end{aligned} \quad (27)$$

$$\begin{aligned} \langle (L+1)^+ || (d^\dagger \tilde{f} + f^\dagger \tilde{d})^1 || L^- \rangle &= -\frac{16n^2 - 12(L+1)n + 3(L-1)(L+2)}{5(2n+1)} \times \\ &\sqrt{\frac{(2n+L+4)L}{28n(2n+3)}}. \end{aligned} \quad (28)$$

(i) $(2n+1,1)K=1 \ L^- \rightarrow (2n-2,2)K=0 \ (L-1)^+$ transitions, e.g. $1^- \rightarrow 0^+$,

$$\begin{aligned} \langle (L-1)^+ || (s^\dagger \tilde{p} + p^\dagger \tilde{s})^1 || L^- \rangle &= -\frac{2n-3L+3}{2n(2n+1)} \times \\ &\sqrt{\frac{(n+1)(2n+L+2)(L+1) \varphi(2n-1, L-1)}{15(2n+3)}}, \end{aligned} \quad (29)$$

$$\begin{aligned} &\langle (L-1)^+ || (d^\dagger \tilde{p} + p^\dagger \tilde{d})^1 || L^- \rangle \\ &= \frac{8n^3 + 12(2L+1)n^2 - 2(L-1)(2L-3)n - 3(L-1)^2(L+3)}{10n(2n+1)} \times \\ &\sqrt{\frac{(n+1)(2n+L+2)(L+1)}{3(2n+3) \varphi(2n-1, L-1)}}, \end{aligned} \quad (30)$$

$$\begin{aligned}
& \langle (L-1)^+ | (d^\dagger \tilde{f} + f^\dagger \tilde{d})^1 | L^- \rangle \\
&= \frac{32n^3 - 24(L-2)n^2 - 2(L-1)(3L-2)n + 3(L-2)(L-1)^2}{10n(2n+1)} \times \\
& \sqrt{\frac{(n+1)(2n+L+2)(L+1)}{7(2n+3) \varphi(2n-1, L-1)}}.
\end{aligned} \tag{31}$$

(j)(2n+1,1)K=1 $L^- \rightarrow (2n-2,2)K=0 L^+$ transitions, e.g. $2^- \rightarrow 2^+$,

$$\begin{aligned}
& \langle L^+ | (s^\dagger \tilde{p} + p^\dagger \tilde{s})^1 | L^- \rangle = -\frac{1}{2n(2n+1)} \times \\
& \sqrt{\frac{(2n-L+2)(n+1)(2n+L+3)(2L+1) \varphi(2n-1, L)}{15}},
\end{aligned} \tag{32}$$

$$\begin{aligned}
& \langle L^+ | (d^\dagger \tilde{p} + p^\dagger \tilde{d})^1 | L^- \rangle = \frac{4n^2 + L^2 + L - 3}{10n(2n+1)} \times \\
& \sqrt{\frac{(2n-L+2)(n+1)(2n+L+3)(2L+1)}{3 \varphi(2n-1, L)}},
\end{aligned} \tag{33}$$

$$\begin{aligned}
& \langle L^+ | (d^\dagger \tilde{f} + f^\dagger \tilde{d})^1 | L^- \rangle = \frac{16n^2 - L^2 - L - 2}{10n(2n+1)} \times \\
& \sqrt{\frac{(2n-L+2)(n+1)(2n+L+3)(2L+1)}{7 \varphi(2n-1, L)}}.
\end{aligned} \tag{34}$$

(k)(2n+1,1)K=1 $L^- \rightarrow (2n-2,2)K=0 (L+1)^+$ transitions, e.g. $1^- \rightarrow 2^+$,

$$\begin{aligned}
& \langle (L+1)^+ | (s^\dagger \tilde{p} + p^\dagger \tilde{s})^1 | L^- \rangle = -\frac{2n+3L+6}{2n(2n+1)} \times \\
& \sqrt{\frac{(n+1)(2n-L+1)L \varphi(2n-1, L+1)}{15(2n+3)}},
\end{aligned} \tag{35}$$

$$\begin{aligned}
& \langle (L+1)^+ | (d^\dagger \tilde{p} + p^\dagger \tilde{d})^1 | L^- \rangle \\
&= \frac{8n^3 - 12(2L+1)n^2 - 2(L+2)(2L+5)n + 3(L-2)(L+2)^2}{10n(2n+1)} \times \\
& \sqrt{\frac{(n+1)(2n-L+1)L}{3(2n+3) \varphi(2n-1, L+1)}},
\end{aligned} \tag{36}$$

$$\begin{aligned}
& \langle (L+1)^+ | (d^\dagger \tilde{f} + f^\dagger \tilde{d})^1 | L^- \rangle \\
&= \frac{32n^3 + 24(L+3)n^2 - 2(L+2)(3L+5)n - 3(L+2)^2(L+3)}{10n(2n+1)} \times \\
& \sqrt{\frac{(n+1)(2n-L+1)L}{7(2n+3) \varphi(2n-1, L+1)}}.
\end{aligned} \tag{37}$$

(l)(2n+1,1)K=1 $L^- \rightarrow (2n-2,2)K=2 (L-1)^+$ transitions, L is odd,
e.g. $3^- \rightarrow 2^+$,

$$\langle (L-1)^+ | (s^\dagger \tilde{p} + p^\dagger \tilde{s})^1 | L^- \rangle = 0, \quad (38)$$

$$\begin{aligned} \langle (L-1)^+ | (d^\dagger \tilde{p} + p^\dagger \tilde{d})^1 | L^- \rangle &= -\frac{1}{5} \sqrt{\frac{3(n+1)(2n+3)(L-2)(L-1)}{2n(2n+1)L}} \times \\ &\sqrt{\frac{(2n-L+1)(2n+L)(2n+L+2)}{\varphi(2n-1, L-1)}}, \end{aligned} \quad (39)$$

$$\begin{aligned} \langle (L-1)^+ | (d^\dagger \tilde{f} + f^\dagger \tilde{d})^1 | L^- \rangle &= -\frac{2}{5} \sqrt{\frac{(n+1)(2n+3)(L-2)(L-1)}{14n(2n+1)L}} \times \\ &\sqrt{\frac{(2n-L+1)(2n+L)(2n+L+2)}{\varphi(2n-1, L-1)}}. \end{aligned} \quad (40)$$

(m)(2n+1,1)K=1 $L^- \rightarrow (2n-2,2)K=2 L^+$ transitions, L is odd,
e.g. $3^- \rightarrow 3^+$,

$$\langle L^+ | (s^\dagger \tilde{p} + p^\dagger \tilde{s})^1 | L^- \rangle = 0, \quad (41)$$

$$\begin{aligned} \langle L^+ | (d^\dagger \tilde{p} + p^\dagger \tilde{d})^1 | L^- \rangle &= -\frac{1}{20n} \sqrt{\frac{6(n+1)(2n+3)(L-1)(L+2)(2L+1)}{(2n+1)L(L+1)}} \times \\ &\sqrt{(2n-L+1)(2n+L+2)}, \end{aligned} \quad (42)$$

$$\begin{aligned} \langle L^+ | (d^\dagger \tilde{f} + f^\dagger \tilde{d})^1 | L^- \rangle &= -\frac{1}{10n} \sqrt{\frac{2(n+1)(2n+3)(L-1)(L+2)(2L+1)}{7(2n+1)L(L+1)}} \times \\ &\sqrt{(2n-L+1)(2n+L+2)}. \end{aligned} \quad (43)$$

(n)(2n+1,1)K=1 $L^- \rightarrow (2n-2,2)K=2 (L+1)^+$ transitions, L is odd,
e.g. $1^- \rightarrow 2^+$,

$$\langle (L+1)^+ | (s^\dagger \tilde{p} + p^\dagger \tilde{s})^1 | L^- \rangle = 0, \quad (44)$$

$$\begin{aligned} \langle (L+1)^+ | (d^\dagger \tilde{p} + p^\dagger \tilde{d})^1 | L^- \rangle &= -\frac{1}{5} \sqrt{\frac{3(n+1)(2n+3)(L+2)(L+3)}{2n(2n+1)(L+1)}} \times \\ &\sqrt{\frac{(2n-L-1)(2n-L+1)(2n+L+2)}{\varphi(2n-1, L+1)}}, \end{aligned} \quad (45)$$

$$\langle (L+1)^+ || (d^\dagger \tilde{f} + f^\dagger \tilde{d})^1 || L^- \rangle = -\frac{2}{5} \sqrt{\frac{(n+1)(2n+3)(L+2)(L+3)}{14n(2n+1)(L+1)}} \times \sqrt{\frac{(2n-L-1)(2n-L+1)(2n+L+2)}{\varphi(2n-1, L+1)}}. \quad (46)$$

(o) $(2n+1,1)K=1 \ L^- \rightarrow (2n-2,2)K=2 \ (L-1)^+$ transitions, L is even,
e.g. $4^- \rightarrow 3^+$,

$$\langle (L-1)^+ || (s^\dagger \tilde{p} + p^\dagger \tilde{s})^1 || L^- \rangle = 0, \quad (47)$$

$$\langle (L-1)^+ || (d^\dagger \tilde{p} + p^\dagger \tilde{d})^1 || L^- \rangle = \frac{1}{20n} \sqrt{\frac{6(n+1)(L-2)(L-1)}{(2n+1)L}} \times \sqrt{(2n-L+2)(2n+L+1)(2n+L+3)}, \quad (48)$$

$$\langle (L-1)^+ || (d^\dagger \tilde{f} + f^\dagger \tilde{d})^1 || L^- \rangle = \frac{1}{10n} \sqrt{\frac{2(n+1)(L-2)(L-1)}{7(2n+1)L}} \times \sqrt{(2n-L+2)(2n+L+1)(2n+L+3)}. \quad (49)$$

(p) $(2n+1,1)K=1 \ L^- \rightarrow (2n-2,2)K=2 \ L^+$ transitions, L is even,
e.g. $2^- \rightarrow 2^+$,

$$\langle L^+ || (s^\dagger \tilde{p} + p^\dagger \tilde{s})^1 || L^- \rangle = 0, \quad (50)$$

$$\langle L^+ || (d^\dagger \tilde{p} + p^\dagger \tilde{d})^1 || L^- \rangle = \frac{1}{5} \sqrt{\frac{3(n+1)(L-1)(L+2)(2L+1)}{2n(2n+1)L(L+1)}} \times \sqrt{\frac{(2n-L)(2n-L+2)(2n+L+1)(2n+L+3)}{\varphi(2n-1, L)}}, \quad (51)$$

$$\langle L^+ || (d^\dagger \tilde{f} + f^\dagger \tilde{d})^1 || L^- \rangle = \frac{2}{5} \sqrt{\frac{(n+1)(L-1)(L+2)(2L+1)}{14n(2n+1)L(L+1)}} \times \sqrt{\frac{(2n-L)(2n-L+2)(2n+L+1)(2n+L+3)}{\varphi(2n-1, L)}}. \quad (52)$$

(q) $(2n+1,1)K=1 \ L^- \rightarrow (2n-2,2)K=2 \ (L+1)^+$ transitions, L is even,
e.g. $2^- \rightarrow 3^+$,

$$\langle (L+1)^+ || (s^\dagger \tilde{p} + p^\dagger \tilde{s})^1 || L^- \rangle = 0, \quad (53)$$

$$\langle (L+1)^+ || (d^\dagger \tilde{p} + p^\dagger \tilde{d})^1 || L^- \rangle = \frac{1}{20n} \sqrt{\frac{6(n+1)(L+2)(L+3)}{(2n+1)(L+1)}} \times \sqrt{(2n-L)(2n-L+2)(2n+L+3)}, \quad (54)$$

$$\langle (L+1)^+ || (d^\dagger \tilde{f} + f^\dagger \tilde{d})^1 || L^- \rangle = \frac{1}{10n} \sqrt{\frac{2(n+1)(L+2)(L+3)}{7(2n+1)(L+1)}} \times \sqrt{(2n-L)(2n-L+2)(2n+L+3)}. \quad (55)$$

C. The M1 transition matrix elements

(a) $(2n+1,1)K=1 \ L^- \rightarrow (2n+3,0)K=0 \ (L-1)^-$ transitions, e.g. $2^- \rightarrow 1^-$,

$$\langle (L-1)^- || (p^\dagger \tilde{p})^1 || L^- \rangle = -\frac{(2n-L+2)(2n+L+3)}{5(2n+1)} \times \sqrt{\frac{3(2n-L+4)(L+1)}{8n(n+1)(2n+3)}}, \quad (56)$$

$$\langle (L-1)^- || (f^\dagger \tilde{f})^1 || L^- \rangle = -\frac{16n^2 + (L-2)(L+3)}{10(2n+1)} \times \sqrt{\frac{3(2n-L+4)(L+1)}{28n(n+1)(2n+3)}}, \quad (57)$$

$$\langle (L-1)^- || (d^\dagger \tilde{d})^1 || L^- \rangle = \sqrt{\frac{3n(2n-L+4)(L+1)}{10(n+1)(2n+3)}}. \quad (58)$$

(b) $(2n+1,1)K=1 \ L^- \rightarrow (2n+3,0)K=0 \ (L+1)^-$ transitions, e.g. $2^- \rightarrow 3^-$,

$$\langle (L+1)^- || (p^\dagger \tilde{p})^1 || L^- \rangle = -\frac{(2n-L+2)(2n+L+3)}{5(2n+1)} \times \sqrt{\frac{3(2n+L+5)L}{8n(n+1)(2n+3)}}, \quad (59)$$

$$\langle (L+1)^- || (f^\dagger \tilde{f})^1 || L^- \rangle = -\frac{16n^2 + (L-2)(L+3)}{10(2n+1)} \times \sqrt{\frac{3(2n+L+5)L}{28n(n+1)(2n+3)}}, \quad (60)$$

$$\langle (L+1)^- || (d^\dagger \tilde{d})^1 || L^- \rangle = \sqrt{\frac{3n(2n+L+5)L}{10(n+1)(2n+3)}}. \quad (61)$$

III. STUDIES OF OCTUPOLE VIBRATION IN ^{152}Sm

A. The spectrum

The spectrum of the spdf SU(3) is compared with data [34] in Fig.1. The parameters are set as: $a_1=-7.49\text{keV}$, $\epsilon_-=4.65\text{MeV}$, $a_3=-8.90\text{keV}$. And a_4 is 16.75keV for the positive parity states and 9.67keV for the negative parity states, respectively. The smaller value of a_4 for the negative parity states reflects an increase of moment of inertia for the negative parity states. This phenomenon has also been found in uranium nuclei [35].

The general agreement between experiment and calculation is quite good. The five bands(3 with positive parity and 2 with negative parity) are all well reproduced. However, as expected, due to the approximate nature of the SU(3) dynamic symmetry in this nucleus, there are discrepancies between them, for instance the degeneracy of β and γ bands is broken in experiment. These detailed structures should be the task of an elaborate numerical studies. Here we are content with the result that the gross structure of the nucleus can be accounted for well by the SU(3) dynamic symmetry.

B. The E1 transition rates

We have applied the results in Sect. 2 and those in Ref. [28] to ^{152}Sm with negative parity states. As for the transition operator, simplicity can be obtained if one choose the transition operator as some generator of the dynamical group. In the sd-pf-IBM, there is no SU(3) generator that can be used as E1 transition operator. However there is an O(10) group generator [17] that can change the parity and can be used as E1 transition operator. However this should not be taken to seriously because the nuclear hamiltonian is a “residual” strong interaction, and the E1 transition is induced by electromagnetic interaction. There is no strong argument that the operator in the hamiltonian and the operator in the transition should have the same form. With our present knowledge, the transition operator should be determined from experimental data. Since a generator form transition operator can sometimes bring simplicity, it is useful to explore if the O(10) generator can achieve some simplification. At first we take the transition operator as the O(10) generator:

$$T(E1)_\mu^1 = e_1 D_\mu^1, \quad (62)$$

where

$$D_{\mu}^1 = \sqrt{\frac{1}{2}}(s^{\dagger}\tilde{p} + p^{\dagger}\tilde{s})_{\mu}^1 - \sqrt{\frac{4}{5}}(p^{\dagger}\tilde{d} + d^{\dagger}\tilde{p})_{\mu}^1 + \sqrt{\frac{7}{10}}(d^{\dagger}\tilde{f} + f^{\dagger}\tilde{d})_{\mu}^1. \quad (63)$$

The calculation values are listed in the column labeled Cal.1 in Table I. The agreement between experiment and calculation is very good, in particular for those transition from 0^- -band to the positive parity states. The effect of the different terms in the transition operator may play different roles, a combination of them may conceal some of the properties of the individual term. For instance, in the SU(3) limit of the sdg-IBM, each term in the E2 transition operator has an $L(L+3)$ dependence, which plays an important role at large L . But this dependence disappears for the SU(3) generator form of the E2 transition operator; this $L(L+3)$ dependence term is concealed, and leads to the reduction of collectivity problem [36,37]. To see the effect of each individual term, we have calculated the reduced matrix elements of sp, dp and df terms respectively. The calculation results of dp term alone are listed in the column labeled Cal.2 in Table I. We found that the experiment could be reproduced well by using solely the dp term in ^{152}Sm . This indicates that the dp term plays a leading role in the E1 transition in the low-lying states of ^{152}Sm . The inclusion of p-boson for the low-lying negative parity states is very important, as has been pointed in Ref. [11–14].

Finally, we used numerical fitting to improve the agreement. The general E1 transition operator is:

$$T(E1)_{\mu}^1 = e_1[(s^{\dagger}\tilde{p} + p^{\dagger}\tilde{s})_{\mu}^1 + \chi_{dp}(p^{\dagger}\tilde{d} + d^{\dagger}\tilde{p})_{\mu}^1 + \chi_{df}(d^{\dagger}\tilde{f} + f^{\dagger}\tilde{d})_{\mu}^1]. \quad (64)$$

Since we have fixed the coefficient of sp term to 1, we can evaluate the relative weights of these three terms through the values of χ_{dp} and χ_{df} . The results have been listed in the column labeled Cal.3 in Table I, and the parameters are $\chi_{dp} = 81.669$, $\chi_{df} = -4.975$. As expected, the value of χ_{dp} evinces that dp term is far more important than sp and df terms.

IV. APPLICATIONS TO OTHER DEFORMED RARE-EARTH NUCLEI

We have expanded our work to other deformed nuclei, namely ^{154}Sm , $^{156-160}\text{Gd}$, $^{160-162}\text{Dy}$, where E1 experimental data are available. The results are shown in Table II together with the experimental data [38–43]. The arrangement of Table II is the same as that in Table I. The parameters e_1 , χ_{dp} and χ_{df} are listed in Table III. The spectra of the nuclei considered here can be well described by the SU(3) dynamic symmetry. Moreover, the E2 transition rates of the positive parity states can also be reasonably well described by the SU(3) dynamic symmetry [44].

From Table II, we can find that the $B(E1)$ values from 0^- band to ground state band in the nuclei studied are all well reproduced. In particular, it is noted that the ratio $B(E1, 1^- \rightarrow 2_{gs}^+)/B(E1, 1^- \rightarrow 0_{gs}^+)$ is approximately 2 in the spdf IBM SU(3) octupole vibration limit. There is because there is a factor \sqrt{L} in the E1 transition matrix element for $L^- \rightarrow (L-1)^+$, and a factor of $\sqrt{L+1}$ in the E1 transition

matrix element $L^- \rightarrow (L+1)^+$. The other factors in the two matrix elements are almost the same for $N \approx 10$. When $L = 1$, it gives a ratio of 2 for the two B(E1) values. This SU(3) octupole vibration property is all satisfied by the 7 nuclei studied in this work. This property can be used to extract the K values for the low-lying 1^- state of deformed nuclei. For the $K^\pi = 1^-$ bandhead, the transition B(E1) to ground state band states is just the opposite, where the transition to 0_{gs}^+ state is stronger than to 2_{gs}^+ state.

In ^{160}Dy , it is noted that the experimental B(E1) values vary over a wide range from 6.8×10^{-3} W.u. to 3.10×10^{-8} W.u., an order of 5 of change! If one fits the transition from $K^\pi = 0^-$ band, then the transition from $K^\pi = 1^-$ band will be too large compared with experimental data. Conversely if one tries to reproduce the transitions from $K^\pi = 1^-$ band, then the transitions from $K^\pi = 0^-$ band will be too small. The same situation occurred also in Ref. [23]. We therefore suggest that the origins of the 1_2^- state which is the bandhead of the $K^\pi = 0^-$ -band, and 2_1^- state which is a member of the $K^\pi = 1^-$ -band are different. They can not be described simultaneously in the spdf IBM. We also noticed that the assignment of the 1_2^- state as a member of $K^\pi = 0^-$ -band is only temporary in experiment [23,43]. If we consider only the transitions from 2_1^- to positive parity states, agreement is obtained.

In ^{158}Gd , there are 7 B(E1) experimental data. The B(E1) values vary over also a wide range from 0.00633 W.u. to 1.21×10^{-5} W.u.. They are all well reproduced by the spdf IBM SU(3) octupole vibration limit. To our present experimental knowledge, we can say that ^{158}Gd is the best nucleus showing the SU(3) octupole vibration dynamical symmetry. We expect that with the development in experiment, other nuclei with this dynamical symmetry will be discovered in other mass regions, for instance in the actinide region.

From Table III, we can find that in other nuclei:(a). both dp and df terms play important roles in these transitions, so we can not acquire the good agreement only by dp term alone. (b). the values of χ_{dp} and χ_{df} change in a relative narrow range, and dp and df terms have almost the same importance in these nuclei, which is different from ^{152}Sm . And the signs of χ_{dp} and χ_{df} remain invariant in a given isotope chain. (c). in the isotopes of Gd, the changes of χ_{dp} and χ_{df} obey the following regularity: with the number of neutron increasing, χ_{df} decreases, however, the absolute value of χ_{dp} increases first, then decreases. In ^{156}Gd , the absolute value of χ_{df} (4.37) is greater than that of χ_{dp} (-1.62), and in ^{160}Gd , the absolute value of χ_{df} (1.61) is less than that of χ_{dp} (-2.08), which implies that dp and df terms may play different roles in different nuclei. In ^{158}Gd , the absolute value of χ_{dp} reaches its maximum. It requires more experimental data in relevant nuclei to check this relationship between the value of χ_{dp} and the number of neutron in a given isotope chain.

From the E1 transition formulae, we found that the E1 transition between 0^- -band and γ -band is zero in the SU(3) limit. However, such transitions occurred in ^{152}Sm , ^{160}Dy . In ^{152}Sm , $B(E1; 4_\gamma^+ \rightarrow 3_1^-) = 3.2 \times 10^{-5}(13)$, this value is very small. A small symmetry-breaking will give a nonzero value for this transition. For

instance if we introduce some mixing between the β and γ band, that is,

$$|\beta\rangle' = a_1|\beta\rangle + a_2|\gamma\rangle, \quad (65)$$

$$|\gamma\rangle' = -a_2|\beta\rangle + a_1|\gamma\rangle, \quad (66)$$

where the apostrophe labeled the new β -band and γ -band. When $|a_2| = 0.0118$, $B(E1; 4_1^+ \rightarrow 3_1^-) = 3.2 \times 10^{-5}$, and because $|a_2|$ is so small that other properties of γ -band could not be disturbed much. However, in ^{160}Dy , $B(E1; 1_1^- \rightarrow 2_\gamma^+) = 0.018(18)$, a very large value. A simple symmetry breaking can not solve this problem. This is another reason that the 1_2^- state in ^{160}Dy may not belong to the $K^\pi = 0^-$ band. In ^{160}Dy , the E1 transition between 3_3^- of possible $K^\pi = 0^-$ -band to γ band are also observed, which confirmed us that this band is not likely the 0^- -band.

Besides absolute B(E1) data, we also compare relative intensities. If one assumes that E1 is dominant in parity changing transitions and ignore higher order transitions, then the transition probabilities and hence the intensities are

$$int \propto E_\gamma^3 B(E1). \quad (67)$$

Using the values of χ_{dp} and χ_{df} obtained in the previous work for the B(E1) value, we have calculated the relative intensities in $^{152,154}\text{Sm}$ [34,38], $^{156,158,160}\text{Gd}$ [39–41], $^{160,162}\text{Dy}$ [41,42]. The experimental data are taken from the references after each nucleus and from Ref. [23,43]. The calculated results are shown in Table IV with experimental data.

From Table IV, we see besides general agreement, there exist serious deviations in $^{152,154}\text{Sm}$: in experiment, the relative intensity from 1^- of $K^\pi = 1^-$ -band to 2_{gs}^+ is much greater than that to 0_{gs}^+ , but in calculation, the situation is reversed. In general, the square of reduced matrix element for transition from 1^- state of the $K^\pi = 1^-$ -band to 0_{gs}^+ is almost as twice as that to 2_{gs}^+ . The calculated ratio of intensities should be of the order of 1. However we noticed that in ^{152}Sm , the transition to 2_{gs}^+ also involves M2 transitions. In the calculation we have just included the E1 contribution. In ^{154}Sm , the identification of 1^- state is only tentative. Experimental measurement of the E1 transition rate from 1^- to 2_{gs}^+ will be very useful for checking this calculation, since in our model there is little freedom to adjust this transition rate.

V. SUMMARY

We have given analytical expressions for E1 and M1 transitions involving low-lying negative parity states in the SU(3) limit. These E1 transition formulae plus those given in Ref. [28] exhaust the whole possibilities of E1 transitions from 0^- and 1^- band to the ground state band, the beta and gamma band. We also applied these analytical results to some deformed rare-earth nuclei to check the SU(3) octupole vibration prediction. Though there have been some deviation, the main features are checked by the experimental data. Some of the discrepancies are expected because of the approximate nature of the dynamical symmetry in real nucleus, for instance the breaking of the beta and gamma band states degeneracies, some small transitions

between gamma band and $K^\pi = 0^-$ band. They can be resolved by symmetry breaking. Some of the discrepancies can not be nailed down at the moment due to lack of experimental data, for instance, the $K^\pi = 0^-$ band identification in ^{160}Dy . Another important issue which remain to be checked by experiment is the anomalous intensity ratio of $K^\pi = 1^-$ bandhead in $^{152,154}\text{Sm}$. Comparing with the sd-f IBM studies of Cottle and Zamfir [23], we see that the agreements of the calculations of the two models with experimental data are of the same quality. In this spdf IBM study, the p boson is very important in these deformed nuclei, even critical in some nucleus, i.e. ^{152}Sm . In the sd-f IBM study, the f boson is most important. From these empirical studies alone, it is not conclusive which model is more appropriate. However, the spdf IBM is more general, and sd-f IBM is only a special case of the spdf IBM. The two calculations can be thought as being two different parameterizations of the spdf IBM. In the sd-f IBM, it can be considered as a special case in which the energy of the p boson is put infinitely high. In the SU(3) octupole vibration limit, the energy of the p boson is put equal to the energy of the f boson. However in view of the simple mathematical structure of spdf IBM, the microscopic studies [14] and the findings by Kusnezov [15], the spdf interacting boson model is one promising model for describing negative parity collective states in even-even nuclei.

VI. ACKNOWLEDGMENTS

The authors acknowledge the support of China National Natural Science Foundation, China State Education Ministry, Fok Ying Tung Education foundation. EG Zhao also acknowledges the support of Advanced Visitors Scheme of Tsinghua University. The authors also thank the referee for expert reading and helpful criticism of the manuscript.

Corrigenda

In table 1 of reference [28], the lines concerning ^{156}Gd should be replaced by

Nucleus	I_i	I_f	$B(E1, I_i \rightarrow I_f)_{cal}(W.u.)$	$B(E1, I_i \rightarrow I_f)_{exp}(W.u.)$
^{156}Gd	1_2^+	0_1^+	0.0025	0.0025(14)
		2_1^+	0.005	0.006(3)

REFERENCES

- [1] S. J. Zhu et al, J. Phys. G 23, L77 (1997).
- [2] S. J. Zhu et al, Chin. Phys. Lett. 14, 569 (1997).
- [3] G. J. Lane, D. B. Fossan, and R. Wadsworth, Phys. Rev. C 57, R1022 (1998).
- [4] J. F. Smith, C. J. Chiara, A. O. Macchiavelli, Phys. Rev. C 57, R1037 (1998).
- [5] C. F. Liang, P. Paris, M. Vergnes, Phys. Rev. C 57, 1145 (1998).
- [6] G. Hackman, R. V. F. Jansseus, T. Nakatsukasa, Phys. Rev. C 57, R1056 (1998).
- [7] M. Yeh, M. Kadi, T. Belgia, Phys. Rev. C 57, R2085 (1998).
- [8] J.F. C. Cocks et al, Phys. Rev. Lett. 78, 2920 (1997).
- [9] C. Fransen et al, Phys. Rev. C57, 129 (1998).
- [10] V. S. Lac, I. Morrison, Nucl. Phys. A 581, 73 (1995).
- [11] C. S. Han, D. S. Chuu, S. T. Hsieh, and H. C. Chiang, Phys. Lett. B 163, 295 (1985).
- [12] J. Engel and F. Iachello, Phys. Rev. Lett. 85, 1126 (1985).
- [13] J. Engel, and F. Iachello, Nucl. Phys. A 472, 61 (1987).
- [14] T. Otsuka, Phys. Lett. B 182, 256 (1986).
- [15] D. F. Kusnezov, *Nuclear collective quadrupole-octupole excitations in the $U(16)$ spdf interacting boson model*, Ph.D. thesis, Princeton University, 1988.
- [16] H. Z. Sun, M. Zhang, and Q. Z. Han, Chin. J. Nucl. Phys. 13, 121 (1991).
- [17] Y. X. Liu, H. Z. Sun, and E. G. Zhao, J. Phys. G 20, 407 (1994).
- [18] F. Iachello and A. Arima, *The Interacting Boson Model* (Cambridge University Press, Cambridge, 1987).
- [19] D. Kusnezov and F. Iachello, Phys. Lett. B 209, 420 (1988).
- [20] H. Mach, W. Nazarewicz, D. Kusnezov et al, Phys. Rev. C 41, R2469 (1990).
- [21] C. E. Alonso, J. M. Arias, A. Frank et al, Nucl. Phys. A 586, 100 (1995).
- [22] P. D. Cottle and N.V. Zamfir, Phys. Rev. C.58, 1500 (1998).
- [23] P. D. Cottle, N. V. Zamfir, Phys. Rev. C 54, 176 (1996).
- [24] A.F. Barfield, J.L. Wood and B.R. Barrett, Phys. Rev. C34, 2001 (1986).
- [25] A.F. Barfield, B.R. Barrett, J.L. Wood and O. Scholten, Ann. Phys. (N.Y.) 182, 344 (1988).
- [26] P.D. Cottle, K.A. Stukey and K.W. Kemper, Phys. Rev. C38, 2843 (1988).
- [27] W. Nazarewicz, S.L. Tabor, Phys. Rev. C45, 2226 (1992).
- [28] G. L. Long, T. Y. Shen, H. Y. Ji, and E. G. Zhao, Phys. Rev. C 57, 2301 (1998).
- [29] J. A. Cizewski, R. F. Casten, G. J. Smith et al, Phys. Rev. Lett. 40, 167 (1978).
- [30] N. Yoshinaga, Y. Akiyama, and A. Arima, Phys. Rev. Lett. 56, 1116 (1986).
- [31] R.F. Casten and D.D. Warner, in Prog. in Part. Nucl. Phys., v9, eds. D. Wilkinson (Pergamon, Oxford 1983) P.311.
- [32] J. D. Vergdos, Nucl. Phys. A 111, 681 (1968).
- [33] G. L. Long, J. Phys. A 28, 6417 (1995).
- [34] A. Artna-cohen, Nucl. Data Sheets 79, 1 (1996).
- [35] G. L. Long, W. L. Zhang, H. Y. Ji, and S. J. Zhu, Science in China, A41, 1296 (1998).
- [36] S.C. Li and S. Kuyucak, Nucl. Phys. A604, 305 (1996).
- [37] G. L. Long, H. Y. Ji, Phys. Rev. C 57, 1686 (1998).
- [38] R. G. Helmer, Nucl. Data Sheets 69, 507 (1993).

- [39] R. G. Helmer, Nucl. Data Sheets 65, 65 (1992).
- [40] R. G. Helmer, Nucl. Data Sheets 77, 471 (1996).
- [41] C. W. Reich, Nucl. Data Sheets 78, 547 (1996).
- [42] R. G. Helmer, Nucl. Data Sheets 64, 79 (1991).
- [43] Table of Isotopes, 8th edition, eds. R.B. Firestone, V.S. Shirley, C.M. Baglin, S.Y.S. Chu, J. Zipkin, John Wiley and Sons Inc. 1996.
- [44] G. L. Long, W. L. Zhang, H. Y. Ji, and J. F. Gao, J. Phys. G 24, 2133 (1998).

TABLES

K^π	I_i	I_f	Cal.1(W.u.)	Cal.2(W.u.)	Cal.3(W.u.)	Exp.(W.u.)
0^-	1_1^-	0_{gs}^+	0.0042	0.0042	0.0037	0.0042(4)
0^-	1_1^-	2_{gs}^+	0.0081	0.00118	0.0099	0.0077(7)
0^-	1_1^-	2_β^+	1.4×10^{-5}	4.3×10^{-3}	4.0×10^{-3}	$1.3(4) \times 10^{-4}$
0^-	3_1^-	2_{gs}^+	0.0055	0.0044	0.0039	0.0081(16)
0^-	3_1^-	4_{gs}^+	0.0067	0.00119	0.0099	0.0082(16)
1^-	2_1^-	2_{gs}^+	0.0015	0.0015	0.0010	0.0027
1^-	2_1^-	2_β^+	3.8×10^{-4}	6.6×10^{-4}	3.3×10^{-4}	5.6×10^{-5}
1^-	2_1^-	2_γ^+	0.0002	0.0042	0.0033	0.011
1^-	2_1^-	3_γ^+	0.00035	0.0072	0.0056	0.0061

TABLE I. B(E1) values in ^{152}Sm

Nucleus	K^π	I_i	I_f	Cal.1(W.u.)	Cal.2(W.u.)	Cal.3(W.u.)	Exp.(W.u.)
^{154}Sm	0^-	1_1^-	0_{gs}^+	0.0062	0.0062	0.0041	0.0062(4)
	0^-	1_1^-	2_{gs}^+	0.0120	0.0163	0.0106	0.0117(26)
	0^-	3_1^-	2_{gs}^+	0.0081	0.0064	0.0045	0.0078(10)
	0^-	3_1^-	4_{gs}^+	0.0099	0.0162	0.0104	0.0093(14)
^{156}Gd	1^-	1_1^-	0_{gs}^+	0.0005	0.0007	0.0018	0.0016(12)
	1^-	1_1^-	2_{gs}^+	0.0004	0.0001	0.0009	0.0020(15)
	1^-	1_1^-	0_β^+	0.00015	0.00040	0.00020	0.00030(24)
	0^-	1_2^-	0_{gs}^+	0.0025	0.0025	0.0029	0.0025(14)
	0^-	1_2^-	2_{gs}^+	0.005	0.006	0.0051	0.006(3)
^{158}Gd	0^-	1_2^-	2_β^+	9×10^{-6}	0.0025	0.0004	0.0007(5)
	0^-	1_2^-	0_{gs}^+	0.0035	0.0035	0.0028	0.0035(8)
	0^-	1_2^-	2_{gs}^+	0.0068	0.0088	0.0056	0.0063(16)
	1^-	3_1^-	2_{gs}^+	0.00047	0.00105	0.00029	0.00033(10)
	1^-	3_1^-	4_{gs}^+	0.00088	0.00009	0.00041	0.00029(8)
	1^-	2_β^+	1_1^-	6.2×10^{-5}	2.6×10^{-5}	1.3×10^{-5}	$6.4(8) \times 10^{-5}$
	1^-	2_β^+	2_1^-	3.16×10^{-5}	5.00×10^{-4}	1.19×10^{-5}	$1.21(5) \times 10^{-5}$
	1^-	2_β^+	3_1^-	2.54×10^{-4}	1.22×10^{-3}	1.11×10^{-5}	$1.89 \times 10^{-4}(24)$
^{160}Gd	0^-	1_1^-	0_{gs}^+	0.0032	0.0032	0.0021	0.0032(9)
	0^-	1_1^-	2_{gs}^+	0.0062	0.0079	0.0041	0.0060(17)
	0^-	3_1^-	2_{gs}^+	0.0042	0.0035	0.0026	0.0016(5)
	0^-	3_1^-	4_{gs}^+	0.0052	0.0077	0.0035	0.0013(4)
^{160}Dy	1^-	2_1^-	2_{gs}^+	1.4×10^{-6}	1.2×10^{-7}	3.10×10^{-8}	$3.10(17) \times 10^{-8}$
	1^-	2_1^-	2_γ^+	1.8×10^{-7}	3.4×10^{-7}	1.89×10^{-7}	$1.89(10) \times 10^{-7}$
	1^-	2_1^-	3_γ^+	3.0×10^{-7}	6.1×10^{-7}	2.49×10^{-7}	$2.49(13) \times 10^{-7}$
	0^-	1_2^-	0_{gs}^+	3.8×10^{-6}	3.8×10^{-7}	7.3×10^{-7}	$3.8(4) \times 10^{-3}$
	0^-	1_2^-	2_{gs}^+	7.4×10^{-6}	9.4×10^{-7}	1.5×10^{-6}	$6.8(5) \times 10^{-3}$
^{162}Dy	0^-	1_1^-	0_{gs}^+	0.0026	0.0026	0.0026	0.0026(4)
	0^-	1_1^-	2_{gs}^+	0.0051	0.0064	0.0060	0.0060(19)

TABLE II. B(E1) values in deformed rare-earth nuclei

Nucleus	e_1	χ_{dp}	χ_{df}
^{152}Sm	0.00101	81.67	-4.98
^{154}Sm	0.00097	83.15	-8.59
^{156}Gd	0.0118	-1.62	4.37
^{158}Gd	0.0136	-3.83	3.68
^{160}Gd	0.0120	-2.08	1.61
^{160}Dy	0.0007	-0.49	-0.56
^{162}Dy	0.0417	-0.75	-0.35

TABLE III. Parameters in E1 transition operator. The unit of e_1 is in $0.28389 A^{1/3} e fm$, which gives the B(E1) in Weissknopf unit.

Nucleus	$E_{level}(keV)$	K^π	I_i	I_f	Cal.	Exp.
^{152}Sm	963	0^-	1_1^-	0_{gs}^+	55.6	82.3(7)
				2_{gs}^+	100	100(2)
				2_β^+	0.24	0.010(3)
				2_{gs}^+	98.2	100(4)
	1041		3_1^-	4_{gs}^+	100	40.4(19)
				4_{gs}^+	100	100(3)
	1221		5_1^-	6_{gs}^+	72	24(3)
				6_{gs}^+	100	100(3)
	1505		7_1^-	8_{gs}^+	51	12
				0_{gs}^+	100	0.85(6)
	1511	1^-	1_2^-	2_{gs}^+	13.3	100(3)
				0_β^+	8.38	0.09(5)
				2_β^+	0.035	1.42(25)
				2_{gs}^+	100	100(11)
	1530		2_1^-	2_β^+	4.55	0.28(4)
				2_γ^+	10.50	13.43(9)
				3_γ^+	5.283	2.127(24)
				2_{gs}^+	100	35.3(3)
	1579		3_2^-	4_{gs}^+	1.15	100(5)
				2_β^+	14.4	6.6(3)
				4_β^+	0.289	1.30(9)
				2_γ^+	2.11	2.07(15)
				4_γ^+	1.2	0.41(5)
				4_{gs}^+	40	67(34)
	1764		5_2^-	6_{gs}^+	100	100(33)
				8_{gs}^+	100	100(3)
	1879	0^-	9_1^-	10_{gs}^+	31	15
				6_{gs}^+	100	82(20)
	1930	1^-	6_1^-	5_γ^+	5.4	100(4)
				6_{gs}^+	100	100(7)
	2004		7_2^-	8_{gs}^+	14	71(24)
				8_{gs}^+	100	100(5)
	2291		9_2^-	10_{gs}^+	32	27(3)
				8_β^+	58	13(4)
				10_{gs}^+	100	100(5)
				12_{gs}^+	62	59(24)
	2641		11_1^-	10_β^+	72	24
				0_{gs}^+	52	65(2)
				2_{gs}^+	100	100(2)
	1012		3_1^-	2_{gs}^+	83	100(2)
				4_{gs}^+	100	60(1)
	1181		5_1^-	4_{gs}^+	100	100(3)
				6_{gs}^+	98	29.0(7)
^{154}Sm	921	0^-	1_1^-	0_{gs}^+	52	65(2)
				2_{gs}^+	100	100(2)
	1012		3_1^-	2_{gs}^+	83	100(2)
				4_{gs}^+	100	60(1)
	1181		5_1^-	4_{gs}^+	100	100(3)
				6_{gs}^+	98	29.0(7)

1476	1^-	1_2^-	0_{gs}^+	100	0.5
			2_{gs}^+	15	100
1515		2_1^-	2_{gs}^+	100	100(19)
			2_β^+	4.1	5.4(12)
1585		3_2^-	2_{gs}^+	100	26.6(25)
			4_{gs}^+	1.6	100(3)
1774		5_2^-	4_{gs}^+	100	40(5)
			6_{gs}^+	2	100(4)

TABLE IV. Comparisons of relative intensities

table IV continued.

Nucleus	$E_{level}(keV)$	K^π	I_i	I_f	Cal.	Exp.
^{156}Gd	1242	1^-	1_1^-	0_{gs}^+	100	97.1(5)
				2_{gs}^+	54	100(10)
				0_β^+	7.0×10^{-6}	0.07(2)
	1276		3_1^-	2_{gs}^+	100	100(2)
				4_{gs}^+	87	44(2)
	1320		2_1^-	2_{gs}^+	100	100(3)
				2_β^+	7.0×10^{-5}	0.21(2)
	1366	0^-	1_2^-	0_{gs}^+	61.1	54.5(3)
				2_{gs}^+	100	100(1)
				2_β^+	0.09	0.08(3)
	1539		3_2^-	2_{gs}^+	100	94(6)
				4_{gs}^+	86	100(6)
	1638	1^-	7_1^-	6_{gs}^+	100	100(3)
				8_{gs}^+	94	≈ 33
	1958		9_1^-	8_{gs}^+	100	100(3)
				10_{gs}^+	82	7(3)
^{158}Gd	977	1^-	1_1^-	0_{gs}^+	100	100(5)
				2_{gs}^+	51	76(4)
	1042		3_1^-	2_{gs}^+	100	100(20)
				4_{gs}^+	76	47.2(9)
	1176		5_1^-	4_{gs}^+	100	100(6)
				6_{gs}^+	75.9	26.7(16)
	1260		2_β^+	1_1^-	5.1	5.1(46)
				2_1^-	2.75	0.56(4)
				3_1^-	2.01	6.9(6)
	1263	0^-	1_2^-	0_{gs}^+	64	68(4)
				2_{gs}^+	100	100(6)
	1403		3_2^-	2_{gs}^+	100	100(6)
				4_{gs}^+	85	85(5)
	1407	1^-	4_β^+	2_β^+	0.002	0.04(1)
				3_1^-	19.9	19.9(12)
				4_1^-	1.29	0.33(2)
	1639	0^-	5_2^-	5_1^-	5.21	6.6(5)
				4_{gs}^+	100	100(8)
^{160}Gd	1224	0^-	1_1^-	6_{gs}^+	61	33(5)
				0_{gs}^+	60.5	65.2(15)
	1290		3_1^-	2_{gs}^+	100	100.0(22)
				2_{gs}^+	100	100(2)
				4_{gs}^+	84	52(2)
	1428		5_1^-	4_{gs}^+	100	100(6)
				6_{gs}^+	55	< 45
	1640		7_1^-	6_{gs}^+	100	28(11)

^{160}Dy	1359	1^-	2_2^-	8_{gs}^+	36	100(22)
				2_{gs}^+	100	100(3)
				2_γ^+	1.00	17.95(12)
				3_γ^+	0.88	11.59(5)
				2_{gs}^+	100	100.0(13)
	1399		3_2^-	4_{gs}^+	83.8	54.7(5)
				2_γ^+	0.43	0.81(3)
				3_γ^+	1.77	0.50(3)
				4_γ^+	0.65	0.26(3)
				4_{gs}^+	100	100(9)
	1535		4_2^-	3_γ^+	0.55	79.8(14)
				4_γ^+	1.22	13.4(6)
				5_γ^+	0.29	19.6(9)
				0_{gs}^+	60	69(14)
				2_{gs}^+	100	100
^{162}Dy	1489	$*0^-$	1_2^-	0_{gs}^+	60	69(14)
	1276	0^-	1_1^-	2_{gs}^+	100	100
				0_{gs}^+	53	52(14)
	1358		3_1^-	2_{gs}^+	100	100(4)
				2_{gs}^+	84	100(30)
	1519		5_1^-	4_{gs}^+	100	46(4)
				4_{gs}^+	100	100(20)
				6_{gs}^+	96	40(8)
	1692	1^-	2_1^-	2_{gs}^+	58	100(3)
				3_γ^+	100	49(6)

FIGURES

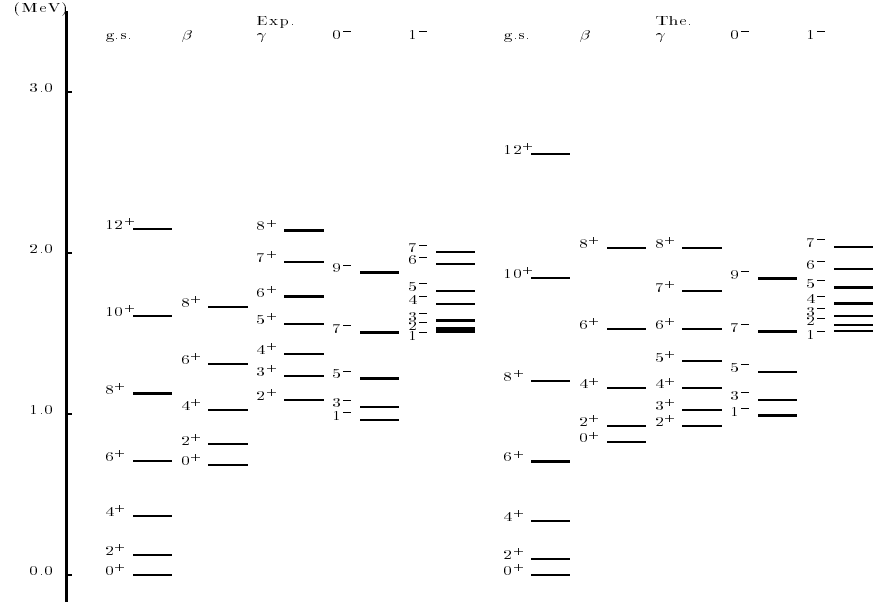


FIG. 1. Spectra of ^{152}Sm .